scientific reports

Check for updates

OPEN

Identification of potential shared gene signatures between periodontitis and breast cancer by integrating bulk RNA-seq and scRNA-seq data

Erli Wu[1,5], Jiahui Liang[2,5], jingxin Zhao[1], Feihan Gu[1], Yuanyuan Zhang[3], Biao Hong[1,4], Qingqing Wang[1,4]✉, Wei Shao[3]✉ & Xiaoyu Sun[1,4]✉

Studies have shown that patients with periodontitis (PD) have an increased risk of breast cancer (BC). However, the exact mechanism remains to be further investigated. This study aimed to investigate the genes, pathways and immune cells that may interact with PD and BC. From the Gene Expression Omnibus (GEO) and TCGA databases, we retrieved the gene expression profiles of samples with PD and BC, respectively. Common genes between two diseases were found using differential expression analysis and weighted gene co-expression network analysis (WGCNA). Machine learning methods were used to find shared diagnostic genes. Single-sample GSEA (ssGSEA) was performed to study the expression profiles of 28 immune cells in PD and BC, and single-cell RNA sequencing (scRNA-seq) data was used to visualize localization of shared genes. Finally, we employed qRT-PCR and immunohistochemistry staining to confirm the expression of hub genes in two diseases. PD and BC had 21 shared crosstalk genes, which were primarily related to peptide hormone response, organic acid transmembrane transport, and carboxylic acid transmembrane transport. By using machine learning methods, ANKRD29 and TDO2 were the most efficient shared diagnostic biomarkers, which were confirmed by Immunohistochemical staining and qRT-PCR. ssGSEA showed that immunology was involved in both diseases and that ANKRD29 and TDO2 may be involved in both diseases by mediating immune cells. scRNA-seq further confirms the importance of these genes in regulating immunity in both diseases. In brief, our study identified 2 genes that may serve as biomarkers and targets for the diagnosis and treatment of PD and BC.

Keywords Periodontitis, Breast cancer, Crosstalk genes, Immune infiltration

Periodontitis (PD) is a common chronic inflammatory and infectious illness characterised by the gradual loss of alveolar bone around the tooth, deterioration of the periodontal ligament and persistent inflammation of the tissues supporting the tooth[1]. Owing to its elevated frequency and occurrence, PD is currently a major global public health concern[2]. Based to epidemiological research, 50% of adults suffer from mild to moderate PD, making it the sixth largest epidemic in human history[3]. Increasing evidence indicates that PD raises the risk of several malignancies, including lung, head and neck, oesophageal and BCs. Numerous bacteria linked to periodontal disease that create a microenvironment favourable for cancer have been isolated from precancerous and cancerous lesions[4]. In addition, the inflammatory process induced by PD can cause oxidative/nitrosative stress through the production of free radicals and reactive intermediates, which may induce DNA mutations or interfere with DNA repair mechanisms and lead to cancer[5].

[1]College & Hospital of Stomatology, Key Lab. of Oral Diseases Research of Anhui Province, Anhui Medical University, Hefei 230032, China. [2]Department of Breast Surgery, Department of General Surgery, The First Affiliated Hospital of Anhui Medical University, 218 JiXi Avenue, Hefei 230022, Anhui, People's Republic of China. [3]Department of Microbiology and Parasitology, Anhui Provincial Laboratory of Pathogen Biology, School of Basic Medical Sciences, Anhui Medical University, Hefei, Anhui, China. [4]Department of Periodontology, Anhui Stomatology Hospital Affiliated to Anhui Medical University, Hefei 230032, China. [5]Erli Wu and Jiahui Liang contributed equally to this work and share first authorship. ✉email: wqq@ahmu.edu.cn; ShaoWei@ahmu.edu.cn; ahmusxy@163.com

Breast cancer (BC) has the highest incidence of malignant tumours among women and is the second leading reason for death globally, accounting for over 2 million newly diagnosed cases and over 60,000 deaths annually[6]. A growing body of evidence suggests that the pathophysiology of BC may be linked to PD and oral microbial dysbiosis. *Porphyromonas gingivalis* (*P. gingivalis*) and *Fusobacterium nucleatum (F. nucleatum)*, two periodontal pathogens, have the ability to activate toll-like receptors on oral epithelial cells. This can lead to an upregulation of the IL-6/signal transducer and activator of transcription 3 (STAT3) pathway, hence promoting carcinogenesis[7]. Additionally, in experimental animal models, *F. nucleatum* in the oral cavity can spread to breast malignancies via the bloodstream, where it accelerates the growth of tumors and promotes the development of metastatic lesions[8]. Meanwhile, many epidemiologic studies have also shown that PD is associated with the risk of BC[9,10]. According to a recent meta-analysis involving 1,73,162 participants, periodontal disease significantly increased the incidence of BC by 1.22 times[11]. Another observational study involving 168,111 people also showed that PD increased the susceptibility to BC (RR = 1.18; 95% confidence interval [CI]: 1.11–1.26; $I^2 = 17.6\%$)[12]. These results indicate that PD and BC may be related; however, the pathological and molecular interactions between the two diseases remain unknown.

In recent years, bioinformatics techniques have been increasingly used to determine the interplay between diseases and identify potential mechanisms of action and co-pathology between illnesses. In the current study, we used bioinformatics techniques to identify common genes that may be involved in crosstalk between PD and BC, and the hub genes were further found using multiple machine learning methods. To learn more about the underlying mechanisms behind the relationships between the two diseases, we looked at the similarities in the amount of immune infiltration and observed correlations between them and hub genes. Finally, these hub genes were further located using single-cell RNA sequencing (scRNA-seq) data and confirmed by qRT-PCR and immunohistochemical staining, indicating that they could be utilised as biomarkers to forecast the incidence of both diseases.

Materials and methods

Data acquisition

From the Gene Expression Omnibus (GEO) database (https://www.ncbi.nlm.nih.gov/geo/), information regarding genes expressed during PD was gathered. GSE16134, comprising 310 gingival papillae (241 "diseased" and 69 "healthy"), was used as a test cohort in the PD dataset, whereas GSE1334, comprising 247 gingival papillae (183 "diseased" and 64 "healthy"), was used as the validation cohort. The gene expression data for BC were obtained from the TCGA database, which contains 113 healthy controls and 1118 BC samples. Additionally, GSE42568, which consisted of 104 cases and 17 healthy controls, was used as a validation dataset for BC. The scRNA-seq database of PD was derived from GSE164241, which included a total of 21 samples, from 8 diseased tissues and 13 healthy controls. The scRNA-seq database of BC was derived from GSE176078 included 26 primary tumors. Details about the datasets used in this study are shown in Supplementary Table 1.

Identification of differentially expressed genes (DEGs)

The R (4.3.1) software was used to normalize and process the downloaded original gene expression matrix, and the R package "limma" was employed to find the DEGs from the GSE16134 and TCGA datasets. DEGs with an adjusted P-value of < 0.05 and $|\log FC|$ of ≥ 0.05 were examined in the GSE16134 dataset, whereas those with an adjusted P-value of < 0.05 and $|\log FC|$ of ≥ 1.0 were examined in the TCGA dataset. A volcano map and a heatmap for differential gene clustering were created using R software.

The weighted gene co-expression network analysis (WGCNA) network construction and module identification

The "WGCNA" package in R was used to construct co-expression networks and a soft threshold was used to ensure the network was scale-free[13] Hierarchical clustering trees were utilized to identify gene modules, and the topological overlap matrix (TOM)-based hierarchical clustering was employed to generate gene modules with robust linkages. Using Pearson's correlation coefficient, the correlations between diseases and modules were assessed, and the module with the highest disease correlation coefficient was chosen. The genes in the module were used for subsequent analysis.

Identification of shared genes and pathway enrichment

The common genes discovered by DEG and WGCNA were exhibited by creating Venn diagrams. The "clusterProfiler" and "org.Hs.eg.db" packages were used to investigate the pathways and functions connected to these genes via Gene Ontology (GO) and Kyoto Encyclopedia of Genes and Genomes (KEGG)[14–16].

Hub gene screening

To filter out the hub genes between diseases with diagnostic significance, two machine learning algorithms were utilized including the least absolute shrinkage and selection operator (LASSO) regression and the random forest (RF) algorithm. LASSO was carried out using the "glmnet" programme to prevent overfitting. The "randomForest" package was used to construct an RF model, and the top five crucial genes were chosen based on their relevance ranking. The intersection of the genes from the two machine learning methods obtained using the "VennDiagram" package was subsequently employed to evaluate the diagnostic value for PD and BC.

Expression levels of candidate biomarkers and their diagnostic utilities

To create boxplots and ascertain the hub gene expression levels in two diseases, the R package "ggplot2" was utilized. Using the "pROC" program, the diagnostic values of hub genes were evaluated by measuring the receiver operating characteristic's (ROC) area under the curve (AUC). The greater the AUC value, which ranged

from 0 to 1, the better the overall test performance. Furthermore, two external datasets, including GSE10334 for PD and GSE42568 for BC, were used to validate these findings.

Kaplan–Meier (KM) survival curve analysis

KM survival curves were used in the Kaplan–Meier plotter (https://kmplot.com/analysis/) to determine the prognostic properties of the hub genes in BC. The median was used to categorise the expression level of each gene into high and low groups; the curves determined the presence or absence of a relationship between the overall survival (OS) of the patients and the expression levels of the genes. Additionally, correlations between these genes and RFS (Relapse-free survival) and DMFS (Disease-free survival) were assessed.

Single-sample GSEA (ssGSEA)

The "GSVA" R package was utilized to assess the infiltration of immune cells in healthy and diseased samples using ssGSEA and gain further insight into the immune system's roles in the diseases. Furthermore, the relationships between putative biomarkers and infiltrating immune cells were examined using the Spearman approach.

scRNA-seq data analysis

The "Seurat" package was performed to analyze the scRNA-seq data, and the "LogNormalize" function was used to normalize the data. Next, we used the "Harmony" package to remove batch effects between different samples according to the official tutorial, and then performed principal component analysis (PCA). The data was clustered according to the Unified Flow Approximation and Projection (UMAP) model, and the "FindAllMarkers" function was used to find out the marker genes of each group. Based on the CellMarker database and known cell type marker genes, the cell types were annotated. Also, the "CellChat" package was used to identify potential interactions between different cells in the pathogenesis of PD and BC[17].

Gingival tissues and BC sample collection

Human gingival tissue was taken from patients diagnosed with PD and healthy controls who underwent gingival resection or crown lengthening during orthodontic or restorative treatment. A total of 16 human gingival tissues, which consisted of 9 cases of inflammatory gingival tissues and 7 controls, were obtained. Additionally, this study comprised 6 BC samples and 6 control samples. Individuals without systemic diseases, those with comprehensive medical records and patients receiving treatment for the first time were included in the study. This study was approved by Anhui Medical University Affiliated Stomatology Hospital Ethics Committee (Ethics number: 2021006).

RNA collection and qRT-PCR

Total RNA was extracted from gingival and breast tissues using the TRIzol reagent (Invitrogen, USA), and two μg of the total RNA were converted to cDNA using the Takara Bio RT Kit (Takara, Tokyo, Japan). The ABI Prism 7500 Real-Time PCR System provided by Applied Biosystems was utilized for qRT-PCR using the Roche SYBR Green Master Mix (Roche Applied Science, Switzerland). GAPDH served as the internal reference for each of the three qRT-PCR tests. The $2^{-\Delta\Delta Ct}$ relative expression technique was used to calculate the findings. Supplementary Table 2 showed the primers used in the qRT-PCR.

Immunohistochemical staining of gingival and breast tissues

Paraffin was used to embed the extracted gingival and breast tissues after preservation in 4% paraformaldehyde. The paraffin-fixed tissues were cut into serial sections and deparaffinised for antigen extraction. Goat serum was applied to the slides, which were then incubated with the antibodies. The sections were counterstained with hematoxylin after the formation of brown precipitate using a 3,3'-diaminobenzidine tetrahydrochloride (DAB) detection kit (ZSGB-Biotech). Image processing software (ImageJ v 1.48) was used to take and process the images.

Statistical analysis

All statistical analyses were performed using R software (4.3.1). The statistical analysis approach of choice for qPCR data was the unpaired t-test, with a P-value of less than 0.05 being deemed significant, and the data was reported as mean ± standard deviation.

Results

Identification of DEGs

A total of 1105 DEGs, of 651 upregulated and 454 downregulated, were identified in the PD data. 2743 DEGs of 1067 upregulated and 1676 downregulated were identified in the BC data. Heatmaps (Figs. 1a, b) displayed the top 30 DEGs for these two illnesses, and volcano maps for the expression patterns of the DEGs in both disorders were shown in Figs. 2c and d. Merging the upregulated and downregulated genes resulted in the identification of 103 genes that were differentially expressed in the two diseases (Figs. 2e, f).

WGCNA network construction and module identification

A good sample clustering was obtained by checking the outliers of the sample clustering and choosing a suitable cutting line threshold. The PD dataset was subjected to a power of $\beta = 5$, whereas the TCGA dataset for BC employed a β value of 6 to ensure the creation of a scale-free network (Figs. 2a-b). The co-expression network built with BC samples included 19 modules, while the network created with PD samples had 5 modules (Figs. 2c-d). The modules most relevant to the disease were obtained by calculating their correlation coefficients (r) and P-values. In the PD dataset, the turquoise module demonstrated the highest positive correlation ($r = 0.66$), and

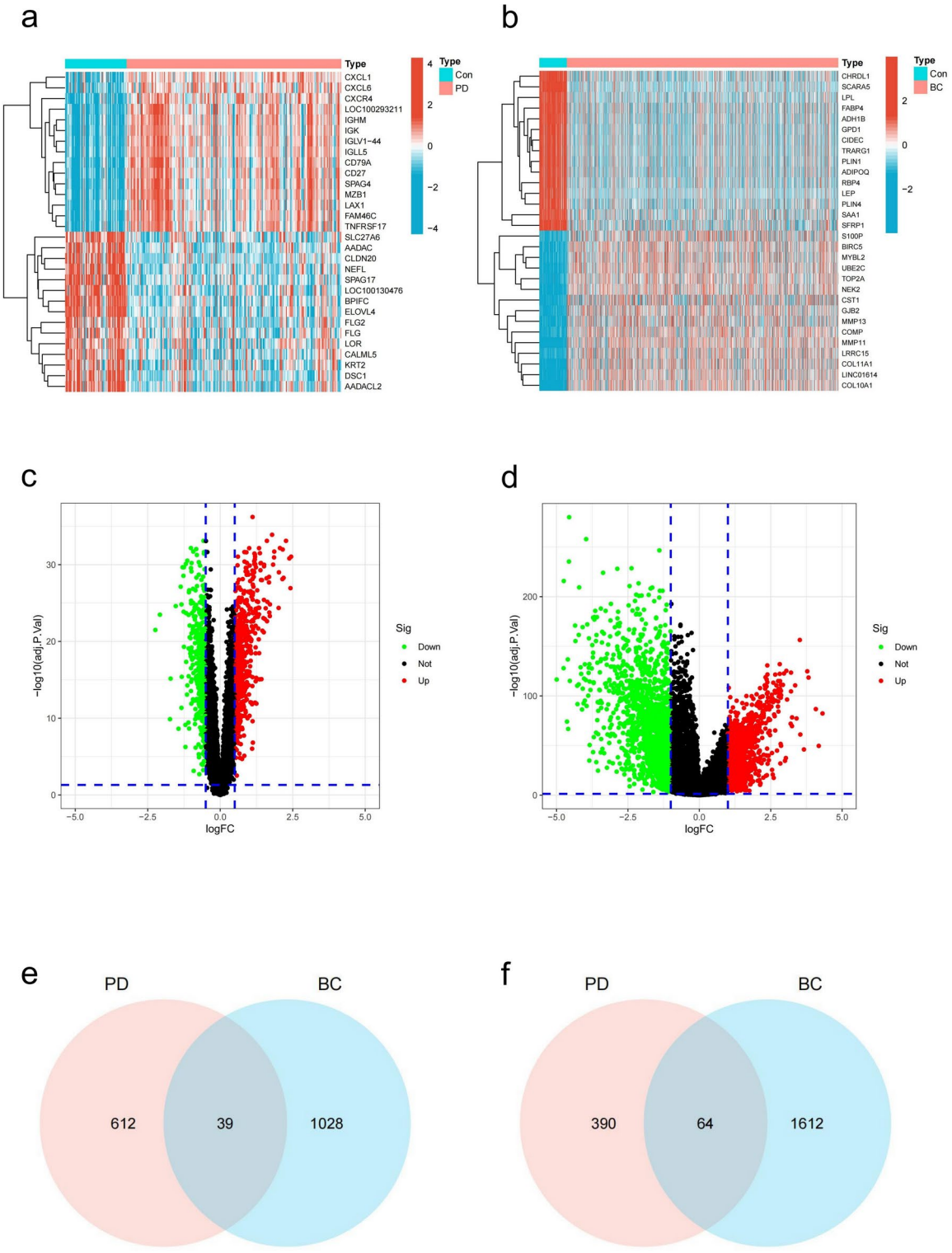

Fig. 1. The identification of genes with variable expression levels. (**a**) Heatmap of the top 30 differentially expressed genes (DEGs) in the PD GSE16134 dataset. (**b**) Heatmap of the top 30 DEGs in TCGA dataset for BC (**c**) Volcano map of the DEGs in the PD dataset GSE16134. (**d**) Volcano map of the DEGs in TCGA dataset for BC. (**e**) Venn diagram showing the overlapping of the upregulated DEGs between the PD and BC data. (**f**) Venn diagram showing the overlapping of the downregulated DEGs between PD and BC data. PD: periodontitis; BC: breast cancer.

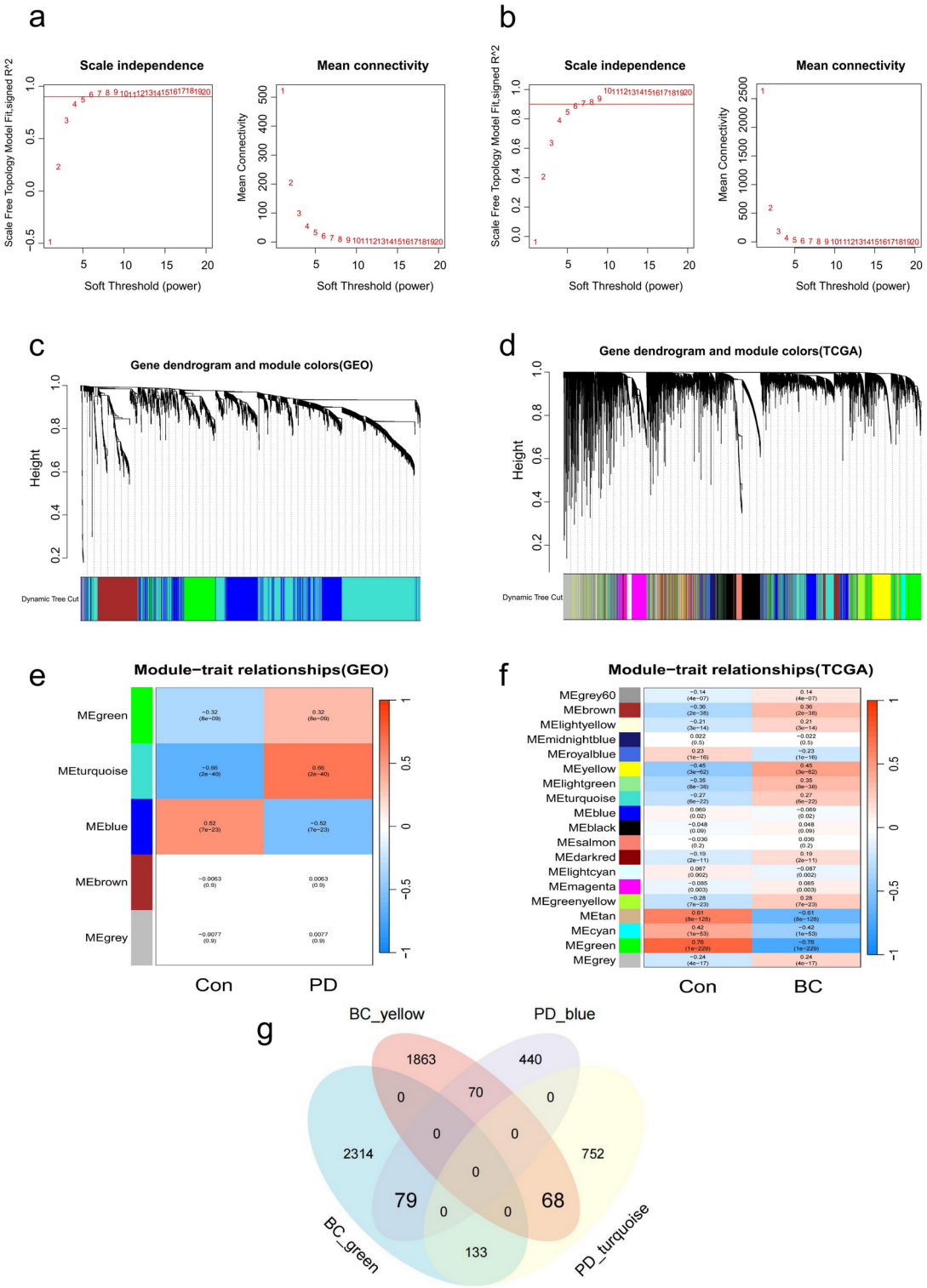

Fig. 2. Analysis of the co-expression of genes with differential expression. (**a**) The optimal soft threshold for the PD GSE16134 database. (**b**) The optimal soft threshold for TCGA dataset for BC. (**c**) The cluster dendrogram for the co-expression of genes in the PD GSE16134 database. (**d**) The cluster dendrogram of co-expressed genes in TCGA dataset for BC. (**e**) Heatmap of the module-trait relationships in the PD GSE16134 database. (**f**) Heatmap of the module-trait connections in TCGA dataset for BC. (**g**) The Venn diagram showed that 147 genes overlapped in the BC and PD modules. PD: periodontitis; BC: breast cancer.

the blue module demonstrated the highest negative correlation (r = -0.52; Fig. 2e). In the BC dataset, the green module exhibited the largest significant negative correlation (r = -0.76), while the yellow module exhibited the strongest positive correlation (r = 0.45; Fig. 2f). By connecting the genes with the highest correlation coefficients in the positive and negative correlation modules, 147 genes in total were found (Fig. 2g).

Identification of shared genes and pathway enrichment

A total of 21 crosstalk genes (TDO2, MARCKSL1, KRT19, SLC7A11, BLM, MMP1, ANKRD29, CYP4F22, ARRDC4, SLC16A7, CD36, CTNNAL1, MAMDC2, CHL1, GNAI1, KAT2B, CTTNBP2, TGFBR3, PLAGL1, GHR and EGR3) for PD and BC were obtained by intersecting the genes in the DEGs and WGCNA using a Venn diagram (Fig. 3a). Evaluations of the functions and pathways of these genes revealed that they were enriched for peptide hormone response, carboxylic acid transport and organic acid transport (Fig. 3b). According to the KEGG database, these genes were mostly involved in growth hormone synthesis, secretion and action, the oestrogen signaling pathway and the chemokine signaling pathway (Fig. 3c).

Screening for hub genes

The LASSO regression and RF algorithm, utilized to find the hub genes common to both disorders, yielded 14 and 5 genes, respectively, in PD-related data (Figs. 3d and e, respectively), and 15 and 5 genes, respectively, in the BC data (Figs. 3f and g, respectively). By intersecting the overlapping genes obtained by the LASSO and RF algorithms in the two diseases, two overlapping genes (ANKRD29 and TDO2) were identified (Fig. 3h).

The expression levels and diagnostic values of the hub genes

Expression levels of two hub genes in PD and BC were displayed by constructing boxplots (Figs. 4a, b). The expression levels of TDO2 were upregulated, and those of ANKRD29 were downregulated in the PD and BC patients, consistent with the results verified by the two external datasets (Figs. 4c, d). The ROC curve for the diagnostic markers revealed that ANKRD29 (AUC = 0.891) and TDO2 (AUC = 0.887) had strong diagnostic values in the GSE16134 dataset (Fig. 4e). Furthermore, ANKRD29 (AUC = 0.968) and TDO2 (AUC = 0.941) demonstrated almost excellent diagnostic values for BC in the TCGA dataset (Fig. 4f). These hub genes were validated using the PD GSE10034 dataset and BC GSE42568 dataset; all of these datasets showed strong predictive performance (Figs. 4g, h).

Prognostic significance of candidate biomarkers

KM curves were used to explore the prognostic implications of these biomarkers for BC. According to the findings, improved OS (HR = 0.65, p = 0.0022), RFS (HR = 0.57, p = 5.1e-13) and DMFS (HR = 0.72, p = 0.015) were linked to greater ANKRD29 levels (Figs. 4i-k). Low TDO2 expression was linked to improved OS (HR = 1.33, p = 0.0041), RFS (HR = 1.17, p = 0.0022) and DMFS (HR = 1.54, p = 8e-08) (Figs. 4l-n). These results suggest that ANKRD29 and TDO2 have prognostic significance for BC.

Immune infiltration analysis

ssGSEA was used to investigate 28 types of immune cell infiltration in various samples. As seen in Figs. 5a and b (boxplots), PD and BC were associated with high levels of activated CD4 T cells, activated CD8 T cells, activated dendritic cells, immature B cells, myeloid-derived suppressor cell (MDSC), regulatory T cells (Tregs) and type 2 T helper (Th2) cells. The immune cell-candidate biomarker connections were analysed to investigate the relationships between the hub genes and the 28 immune cells. TDO2 positively controlled the majority of immune cells in both the PD and BC samples, such as activated CD4 T cells, Tregs and MDSCs. ANKRD29 correlated positively with most immune cells in BC and negatively with most immune cells in PD (Figs. 5c, d). These findings imply that TDO2 and ANKRD29 may control immune cells to affect the development of PD and BC.

scRNA-seq analysis for hub genes

Firstly, the quality control and data processing of the RNA-seq data GSE164241 and GSE176078 were carried out. For PD dataset GSE164241, the annotation of cell surface markers yielded a total of 11 distinct cell types, including endothelial cells, NK/T cells, B cells, fibroblasts, plasma B cells, vascular murals, epithelial cells, myeloid cells, mast cells, proliferative cells and melanocytes (Fig. 6a). Figure 6b illustrated the expression of known lineage markers in 11 major cell clusters in the normal and PD groups. The results of localization of the gene showed that ANKRD29 was mainly located in fibroblasts, vascular murals and endothelial cells in gingival tissue, and the expression of ANKRD29 in PD samples was decreased compared with that in normal samples. TDO2 was mainly located in fibroblasts and vascular murals, and the expression of TDO2 in PD samples was higher than that in normal samples (Fig. 6c). These results were consistent with bulk transcriptomic results. For BC dataset GSE176078, the annotation of cell surface markers yielded a total of 9 distinct cell types, including B cells, cancer-associated fibroblasts (CAFs), cancer epithelial cells, endothelial cells, myeloid cells, normal epithelial cells, plasmablasts, perivascular-like (PVL) cells and T cells (Fig. 6d). Figure 6e illustrated the expression of known lineage markers in 9 major cell clusters in BC samples. It was demonstrated that TDO2 was primarily found in cancer epithelium, PVL cells, and CAFs, whereas ANKRD29 was primarily found in endothelial and PVL cells in BC (Fig. 6f). To further explore the role of hub genes in PD and BC, we divided the cells mainly expressed by hub genes into negative and positive populations according to the expression of hub genes. In PD, ANKRD29 + endothelial cells had a stronger output signal than ANKRD29- endothelial cells (Fig. 7a). Compared with TDO2- fibroblasts, TDO2 + fibroblasts had stronger incoming and outgoing signals (Fig. 7b). In addition, in BC, both ANKRD29^{+} endothelial cells and TDO2 + cancer epithelial cells had stronger incoming and outgoing signals than their negative cells (Figs. 7c-d). Figures 7e-h specifically revealed the role

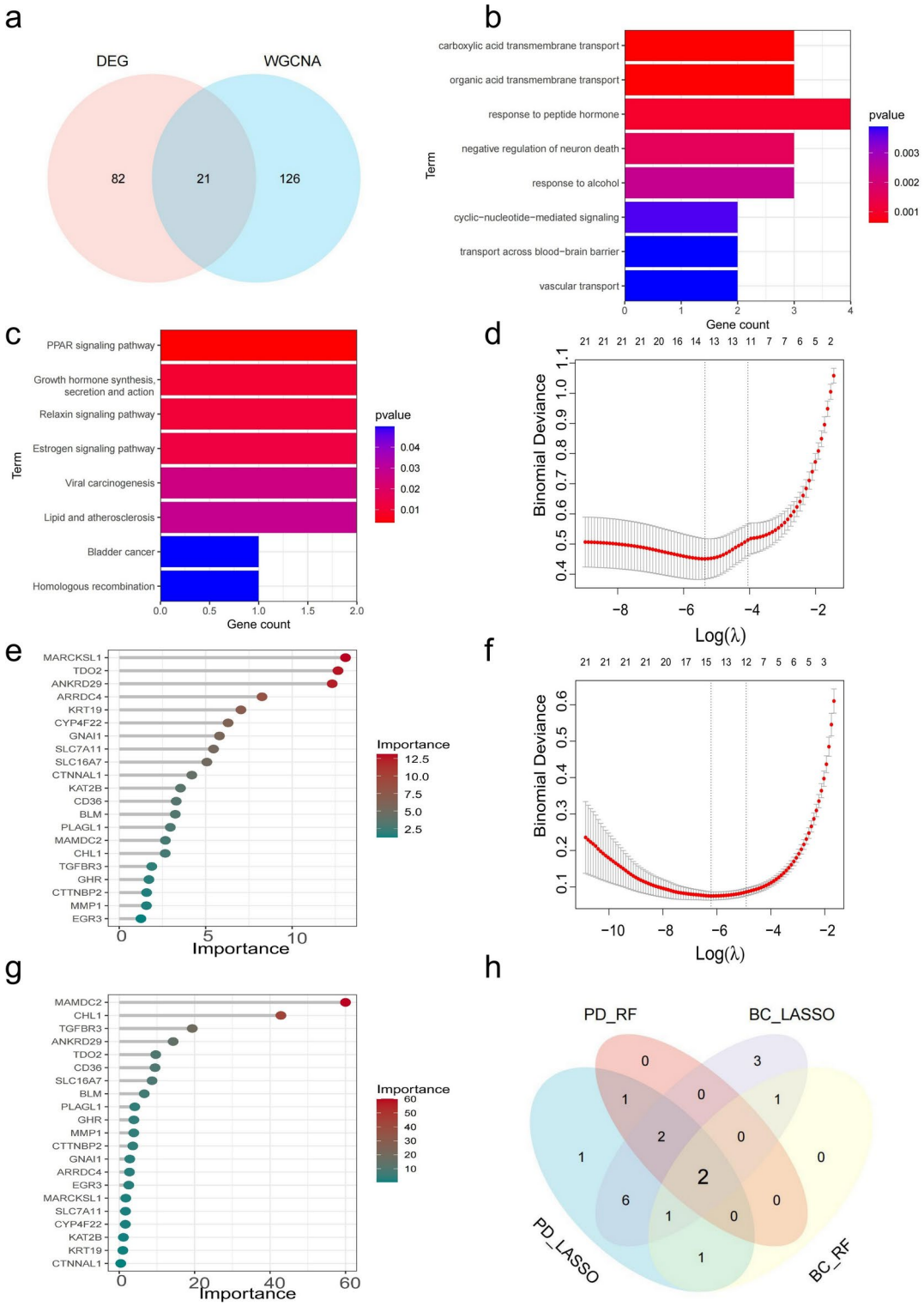

Fig. 3. Identification of the hub genes using machine learning methods. (**a**) Venn diagram showing the 21 genes selected from the union set between the DEGs and trait-module key genes in WGCNA. (**b**) GO analysis of the shared genes. (**c**) KEGG pathway enrichment analysis of the shared genes. (**d**-**e**) LASSO and RF algorithms were conducted to determine the hub genes in PD. (**f**-**g**) LASSO and RF algorithm were conducted to determine the hub genes in BC. (**h**) Venn diagram showing the shared hub genes for PD and BC. PD: periodontitis; BC: breast cancer; DEG: differentially expressed gene; WGCNA: weighted gene co-expression network analysis; LASSO: least absolute shrinkage and selection operator; RF: random forest.

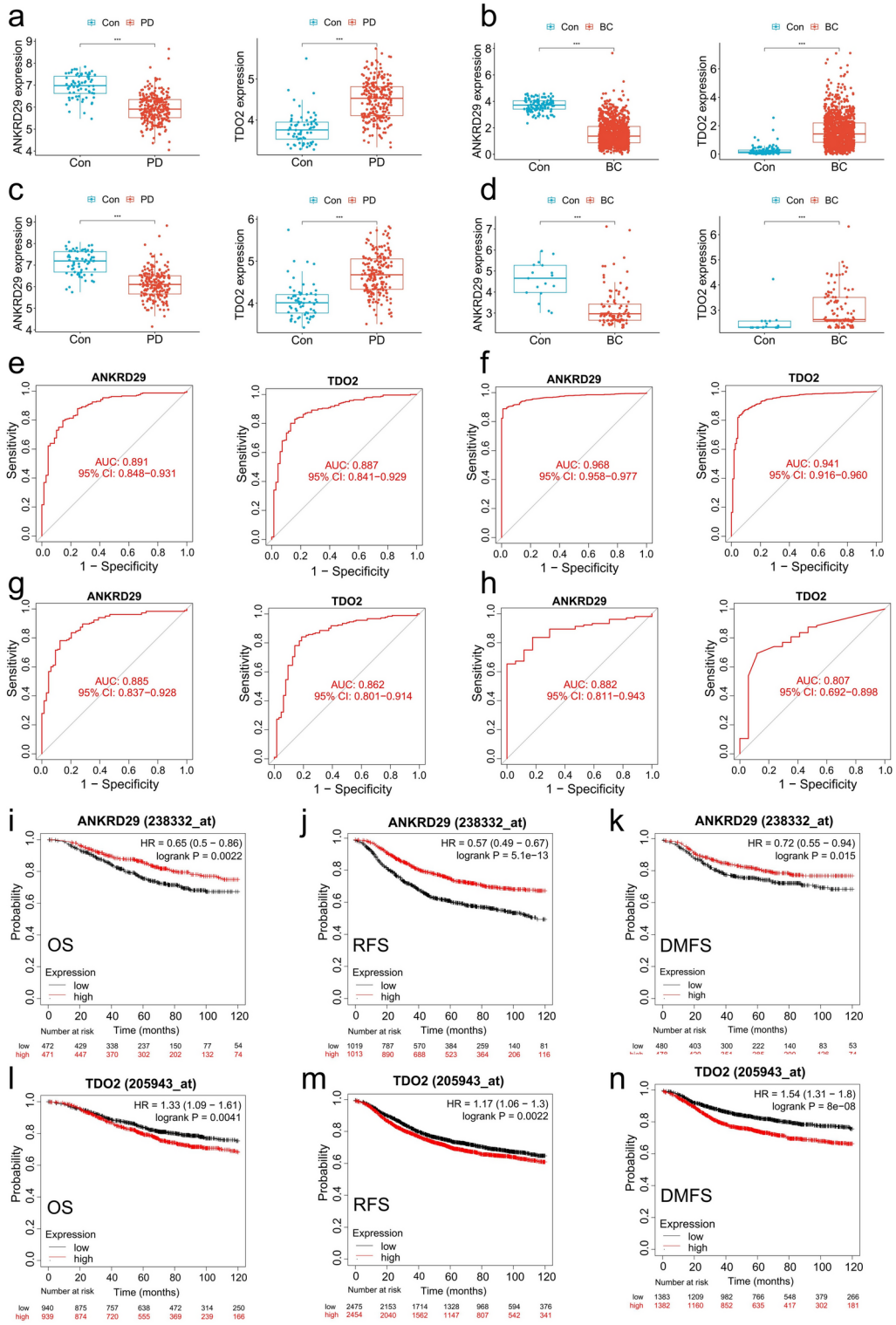

Fig. 4. Validation of the expression pattern and the diagnostic and prognostic value. (**a**) The expression of ANKRD29 and TDO2 in the PD GSE16134 database. (**b**) The expression of ANKRD29 and TDO2 in TCGA dataset for BC. (**c**) The expression of ANKRD29 and TDO2 in the PD validation GSE10334 database. (**d**) ANKRD29 and TDO2 expression in the BC validation GSE42568 database. (**e**) ROC curve of the shared diagnostic genes in GSE16134. (**f**) ROC curve of the shared diagnostic genes in TCGA dataset for BC. (**g**) ROC curve of the shared diagnostic genes in GSE10334. (**h**) ROC curve of the shared diagnostic genes in the BC validation GSE42568 dataset. (**i-k**) OS, RFS, DMFS between the high-low ANKRD29 gene expression groups in the Kaplan–Meier Plotter. (**l-n**) OS, RFS, DMFS between the high-low TDO2 gene expression groups in the Kaplan–Meier Plotter. PD: periodontitis; BC: breast cancer; Con: control; OS: Overall survival; RFS: Relapse-free survival. DMFS: Distant metastasis-free survival. *P < 0.05; **P < 0.01; ***P < 0.001.

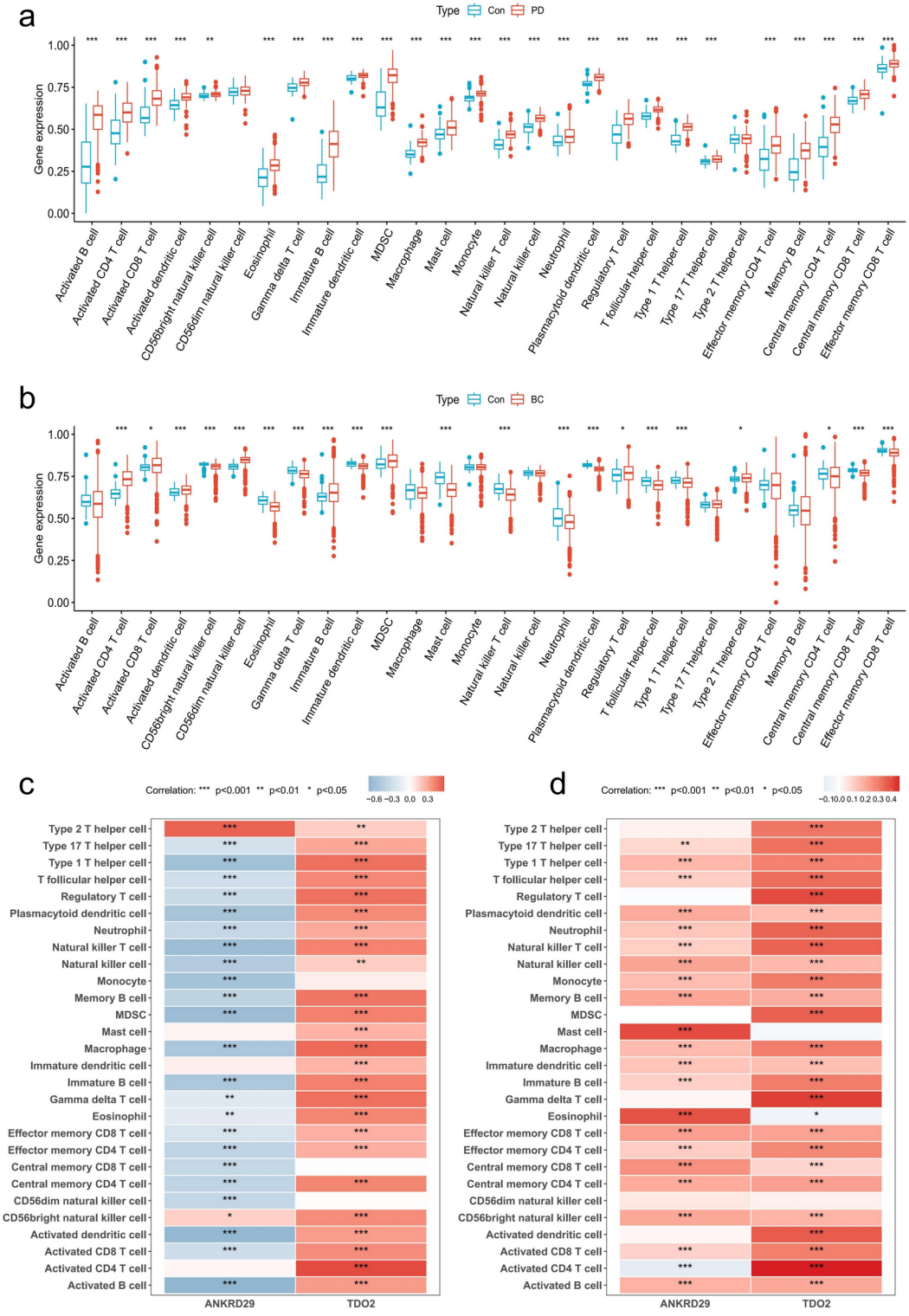

Fig. 5. Analysis of the immune infiltration associated with PD and BC. (**a**) A boxplot of the distribution of 28 immune cells in normal and PD samples. (**b**) A boxplot of the distribution of 28 immune cells in normal and BC samples. (**c**) The relationship between the hub genes and immune cell infiltration in the PD GSE16134 dataset. (**d**) The relationship between hub genes and immune cell infiltration in TCGA dataset for BC. PD: periodontitis; BC: breast cancer; Con, control.

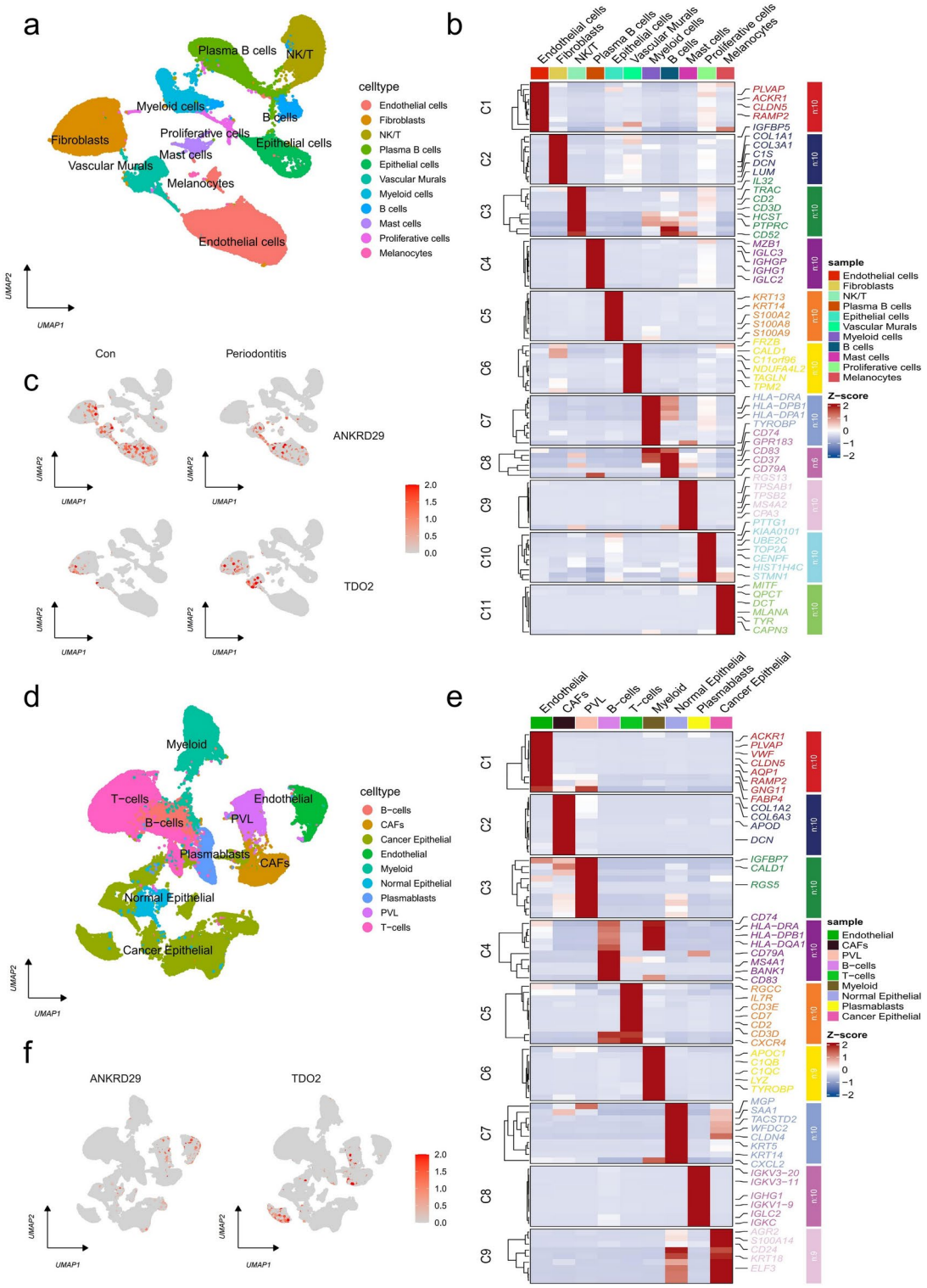

Fig. 6. Single-cell analysis of cell proportions of PD and BC. (**a**) UMAP plot visualizes the distribution of 11 cell types in gingival sample. (**b**) Heatmap showing representative DEGs between each cell population. (**c**) ANKRD29 and TDO2 expression levels in 11 main cell clusters of Con group and PD group. (**d**) UMAP plot visualizes the distribution of 9 cell types in BC. (**e**) Heatmap showing representative DEGs between each cell population. (**f**) ANKRD29 and TDO2 expression levels in 9 main cell clusters of BC. PD: periodontitis; BC: breast cancer; Con, control.

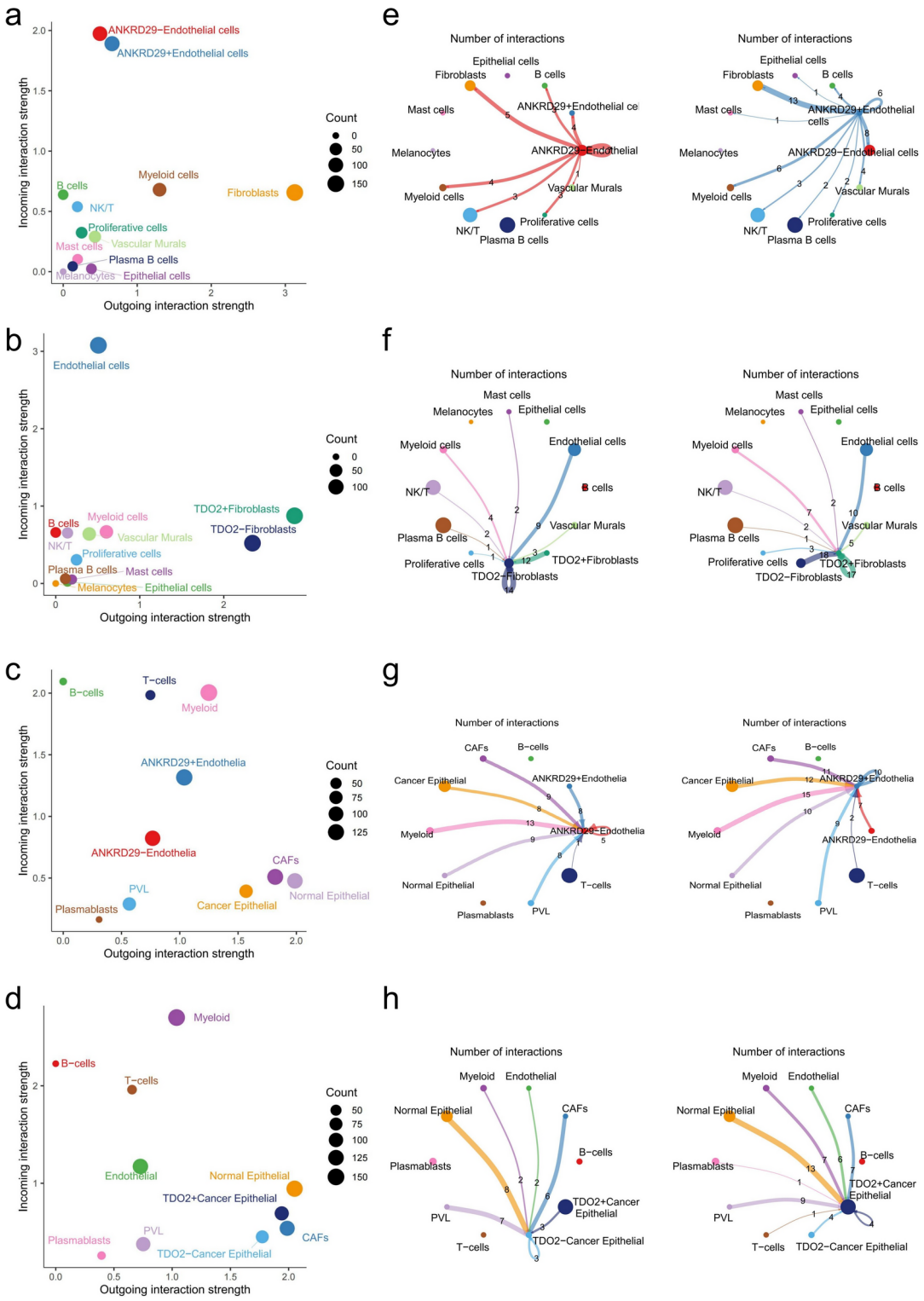

Fig. 7. Cell communication analysis in PD and BC. (**a-b**) Scatter plot of the variations in incoming and outgoing interaction strengths of ANKRD29 and TDO2-related cell types in PD. (**c-d**) Scatter plot of the variations in incoming and outgoing interaction strengths of ANKRD29 and TDO2-related cell types in BC. (**e**) Circos plots showing the interactions density when ANKRD29-associated cells act as transmitters. (**f**) Circle diagram showing cellular communication when TDO2-associated cells act as receptors. (**g**) Circos plots showing the interactions density when ANKRD29-associated cells act as receptors. (**h**) Circos plots showing the interactions density when TDO2-associated cells act as receptors. PD: periodontitis; BC: breast cancer; Con, control.

of related cell subsets in cellular communication in both diseases. It can be seen that compared with subgroups related to negative gene expression, the communication ability between positive gene expression subgroups and immune cells was significantly enhanced. The above-mentioned results suggested that ANKRD29 and TDO2 may play an important role in the pathogenesis of PD and BC.

qPCR and immunohistochemistry

qPCR and immunohistochemistry were used to confirm the expression levels of two potential markers in PD and BC samples and validate their diagnostic values. The results of qRT-PCR revealed that expressions of pro-inflammatory cytokines (IL-1, IL-6 and IL-8) in PD patients were higher than those in healthy controls, indicating the reliability of the sample collection (Fig. 8a). In addition, PD patients had higher levels of TDO2 and lower levels of ANKRD29 compared to healthy controls (Fig. 8b). Similarly, TDO2 mRNA levels were higher in the BC patients, whereas ANKRD29 mRNA levels were lower than those in adjacent normal tissues (Fig. 8c). Based on immunohistochemistry, TDO2 expression was upregulated and ANKRD29 expression was downregulated in PD and BC samples compared to healthy controls (Fig. 8d).

Discussion

There is mounting evidence that some features of PD might affect the course of cancers, such as colorectal, gastric and oral cancers[18–20], implying a connection between PD and cancer. The present investigation merged the transcriptomes of PD and BC, and employed WGCNA to examine the presence of a crosstalk mechanism between the two diseases and to analyse the genes involved in this crosstalk.

The main genes implicated in the crosstalk between PD and BC were associated with carboxylic acid transmembrane transport, organic acid transmembrane transport and peptide hormone response. Carboxylic acids, including fatty acids, lactate, and amino acid derivatives, play essential roles in cellular metabolism, immune responses, and tumor progression. In PD, chronic inflammation alters local metabolic conditions, leading to increased production of organic acids such as lactate and short-chain fatty acids (SCFAs) by periodontal pathogens including *P. gingivalis* and *F. nucleatum*[21]. These metabolites modulate immune cell activity and contribute to systemic inflammation, which may influence the tumor microenvironment in BC[22]. In BC, increased carboxylic acid and organic acid transport is associated with tumor cell metabolism and survival, particularly under hypoxic conditions. For example, lactate transporters (MCT1/4, SLC16A family) enable cancer cells to adapt to metabolic stress, promoting tumor progression and immune evasion[23,24]. SCFAs and other organic acids generated in PD may enter systemic circulation, impacting immune cell polarization including M2 macrophages and Tregs, thereby promoting an immunosuppressive environment conducive to BC progression[25,26]. Dysregulated organic acid transport in PD may contribute to metabolic reprogramming in immune and stromal cells, reinforcing a pro-inflammatory and tumor-promoting microenvironment. Peptide hormones such as leptin, insulin, and adiponectin are known to play crucial roles in both PD and BC, especially with regard to inflammation, immune modulation, and tumorigenesis. PD, as a chronic inflammatory disease, results in the increased release of pro-inflammatory cytokines and hormones like leptin, which can exacerbate tissue destruction and influence systemic inflammation[27]. In parallel, elevated leptin levels in BC have been associated with increased tumor cell proliferation and metastasis[28]. Furthermore, insulin resistance, another feature often seen in PD, has been implicated in BC progression[29,30]. Thus, the inflammation-driven hormonal imbalances caused by PD may contribute to the development and progression of BC.

Accumulated evidence shows that immune cells are involved in inflammatory diseases and in mediating the occurrence, development, invasion and metastasis of tumours through their influence on the tumour microenvironment[31,32]. Furthermore, the type and extent of immune cell invasion are directly linked to the clinical outcomes of the patients[33–35]. Thus, it is crucial to investigate immune cell infiltration and determine how it relates to distinctive hub genes in order to comprehend the process behind PD-induced BC. In this work, we explored the expression levels and dynamic regulation mechanisms of 28 immune cell types in PD and BC using ssGSEA. The results showed that several immune cells were highly expressed in PD and BC, including activated CD4 T cells, activated CD8 T cells, immature B cells, MDSCs, activated dendritic cells, Tregs and Th2 cells. Increased numbers of activated CD4 T cells have been detected in mice with early gingival inflammation, and these activated CD4 T cells could induce osteoclast differentiation by expressing RANKL, thus worsening bone loss in PD patients[36]. In the late stage of *P. gingivalis* infection, CD4 T cells can differentiate into Tregs, which affect alveolar bone metabolism and inhibit the immune response by secreting IL-10 and TGF-β, thereby aiding tumour progression[36–38]. Furthermore, an imbalance in the T lymphocyte ratio was reported to modify the tumour's immune microenvironment, thereby encouraging the growth, invasion and metastasis of tumour cells[39]. In another study, *F. nucleosomes* increased the number of Tregs, leading to advanced tumour growth by preventing cytotoxicity and effector T cells, thus lowering the local anti-tumour immunity[40]. *P. gingivalis* can promote the production of M2 macrophages by modulating the Th2 cell-mediated anti-inflammatory response and inducing immunosuppression to further promote tumour progression[5,41]. Dendritic cells engulf *P. gingivalis* and do not eliminate them, thus allowing these intracellular bacterial cells to travel to distant organs[42]. Furthermore, MDSCs appear to be crucial to the pathophysiology of BC caused by PD. The expansion of MDSCs and their accumulation in malignant lesions is one of the main causes of cancer progression[43]. MDSCs are believed to be most likely to restore homeostasis after inflammation and encourage immunosuppression through the depletion of amino acids required for T-cell activation and proliferation, such as arginine and cysteine, which favour tumour cell growth[44]. Emerging evidence suggests that MDSCs may be involved in PD-induced cancer. An inflammatory response caused by *P. gingivalis* infection can lead to the expansion, activation and recruitment of MDSCs, which can lead to BC metastasis[45,46]. In addition to *P. gingivalis*, *F. nucleosomes* can also recruit MDSCs by increasing the levels of programmed death- ligand 1 (PD-L1), cluster of differentiation 47 (CD47), and upregulation of matrix metallopeptidase 9 (MMP-9), thus promoting BC growth[44]. The aforementioned

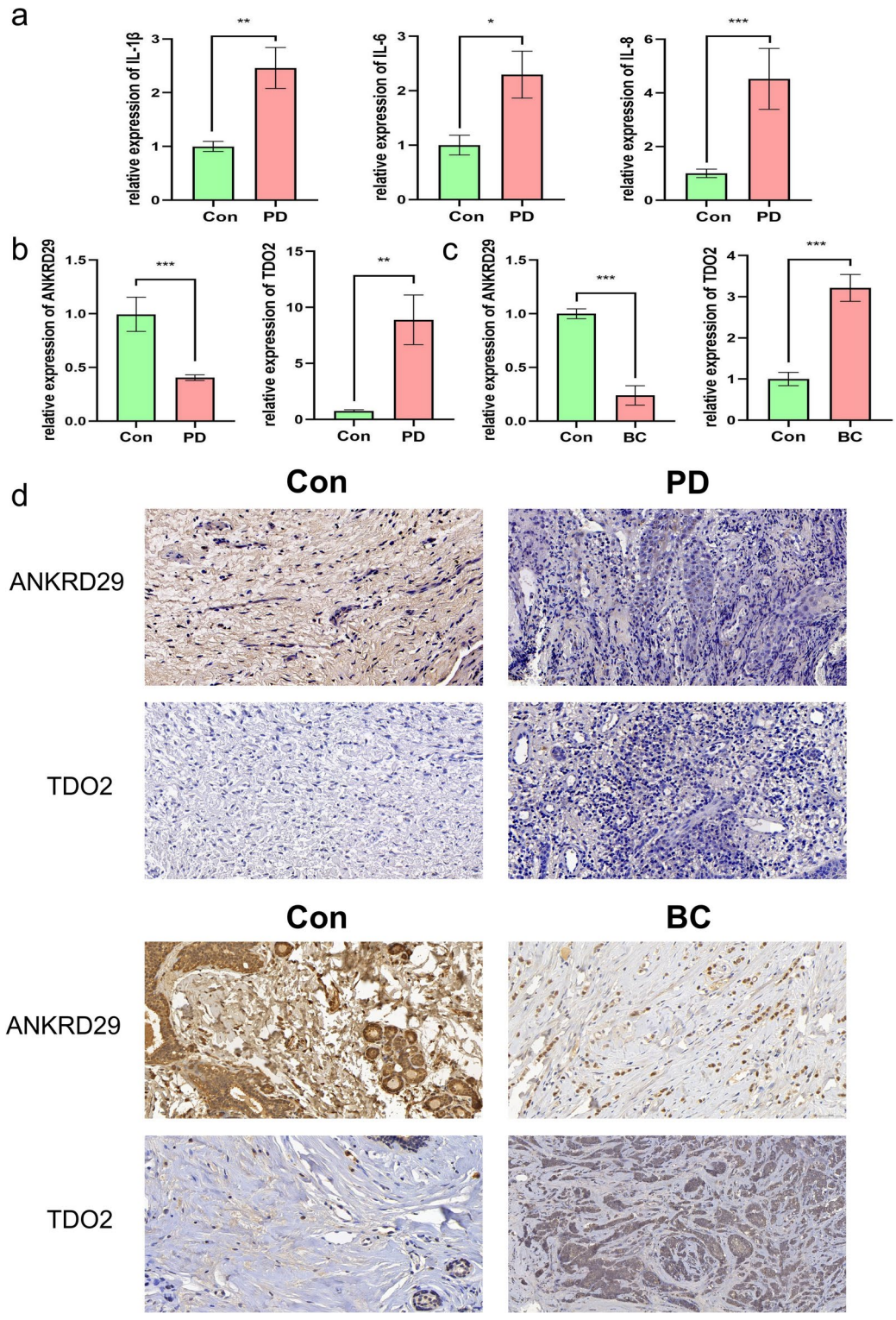

Fig. 8. Expression of ANKRD29 and TDO2 in patients with PD, BC and controls. (**a**) qRT-PCR results show the mRNA expression levels of IL-1β, IL-6 and IL-8 in the gingivae of individuals in the healthy and PD groups ($n_{con} = 7$, $n_{case} = 9$, respectively). GAPDH was used for normalisation relative to the control group. (**b**) qRT-PCR results show the mRNA expression levels of ANKRD29 and TDO2 in the gingivae of individuals in the healthy and PD groups ($n_{con} = 7$, $n_{case} = 9$, respectively). GAPDH was used for normalisation relative to the control group. (**c**) qRT-PCR results show the mRNA expression of ANKRD29 and TDO2 in adjacent normal tissues and BC tissues ($n_{con} = 6$, $n_{case} = 6$). GAPDH was used for normalisation relative to the control group. (**d**) Immunohistochemistry staining of ANKRD29 and TDO2 in the gingivae of individuals in the healthy and PD groups and in BC and healthy tissues. PD: periodontitis; BC: breast cancer; Con, control.

evidence emphasises that PD and BC have similar immune-related pathophysiological characteristics, which may be important to comprehend the connection between the two conditions.

This study identified TDO2 and ANKRD29 as potential biomarkers for PD and BC. The diagnostic and prognostic value of these biomarkers was assessed using ROC and Kaplan–Meier (KM) curves, and further validated by qPCR and immunohistochemistry. Tryptophan 2,3-dioxygenase (TDO2) is a key enzyme in the kynurenine pathway and plays a pivotal role in tryptophan metabolism[47,48]. Elevated TDO2 expression in PD has been linked to systemic immune modulation. In BC, overexpression of TDO2 depletes tryptophan in the tumor microenvironment, which subsequently activates the aryl hydrocarbon receptor (AHR) pathway[48]. This activation suppresses the anti-tumor immune response by promoting Treg differentiation and impairing the proliferation of effector T cells. Furthermore, the accumulation of kynurenine metabolites may directly promote tumor growth and metastasis by enhancing cell survival and angiogenesis[49]. Previous studies have demonstrated that periodontal pathogens, such as *P. gingivalis* and *F. nucleatum*, can enhance the recruitment of Tregs and MDSCs, thereby reducing local anti-tumor immunity and promoting systemic immune suppression[45]. Our findings indicate that TDO2 expression correlates positively with immunosuppressive cells, such as MDSCs and Tregs, in both PD and BC, further supporting its role in mediating an immunosuppressive crosstalk.

ANKRD29 is a member of the ankyrin repeat domain-containing protein family, which plays a critical role in initiating immunological responses and regulating essential cellular functions, including apoptosis, proliferation, migration, epithelial-mesenchymal transition (EMT), and drug sensitivity[50–52]. Studies have established a link between ANKRD29 expression and prognosis in non-small-cell lung cancer (NSCLC) patients. Overexpression of ANKRD29 inhibits tumor progression in NSCLC by suppressing tumor cell growth, migration, and EMT, as well as enhancing drug sensitivity and the cytotoxic activity of T cells[53]. Additionally, decreased expression of ANKRD29 correlates with a poorer prognosis in BC patients ($P = 0.0371$), which aligned with our findings[54]. scRNA-seq data indicated that ANKRD29 was predominantly expressed in endothelial cells and PVL cells in BC and in fibroblasts and endothelial cells in PD. These cell types are crucial for immune surveillance, vascular homeostasis, and inflammatory response. Cell communication analysis revealed stronger interactions between ANKRD29-endothelial cells and neutrophils, macrophages, and T cells in PD. The loss of ANKRD29 expression may contribute to an excessive inflammatory response, leading to chronic inflammation, which is a known risk factor for cancer development. Furthermore, correlation between ANKRD29 and immune cells in PD suggested that the loss of ANKRD29 may facilitate the recruitment and activation of immunosuppressive cells, such as MDSCs and Tregs, thus fostering an immunosuppressive microenvironment that supports cancer cell survival and metastasis. In summary, our findings identify two common biomarkers (TDO2 and ANKRD29) shared between PD and BC that may play a pivotal role in disease development by regulating immune responses and the tumor microenvironment. We propose a potential synergistic mechanism. In PD, chronic inflammation induces immune imbalance, characterized by the downregulation of ANKRD29 and upregulation of TDO2, which leads to excessive immune activation. This, in turn, activates MDSCs and Tregs, both of which contribute to systemic immune suppression and impair the immune system's ability to eliminate cancer cells. In BC, the downregulation of ANKRD29 further disrupts immune surveillance, while the upregulation of TDO2 activates the kynurenine pathway, promoting the development of an immunosuppressive tumor microenvironment.

This study indicated that ANKRD29 and TDO2 are promising potential targets for the treatment of PD and BC. TDO2 is upregulated in both PD and BC, and therapeutic strategies aimed at inhibiting TDO2 may help restore anti-tumor immunity while mitigating chronic inflammation associated with PD. Several TDO2 inhibitors, such as Indoximod and LM10, have demonstrated the ability to restore T cell proliferation and enhance anti-tumor immune responses[55,56]. Furthermore, TDO2-mediated immune suppression occurs through kynurenine-AHR signaling, suggesting that combining TDO2 inhibitors with PD-1/PD-L1 blockade therapies may enhance anti-tumor immunity in BC patients with chronic inflammation. Future studies should aim to establish a systemic model of PD combined with BC to assess the effect of TDO2 inhibitors on restoring anti-tumor immunity and reducing PD-associated systemic inflammation. The downregulation of ANKRD29 in both PD and BC suggests its role in maintaining immune balance. Given its association with endothelial function, fibroblast-mediated immune modulation, and immune cell infiltration, therapies aimed at restoring ANKRD29 expression or modulating its downstream pathways could help correct immune dysregulation in both diseases. Given the lack of direct pharmacological agents targeting ANKRD29, gene therapy strategies, such as Adeno-associated virus (AAV)-mediated gene delivery and CRISPR-based gene activation, could be explored to restore its expression in PD-affected tissues and BC tumors. Furthermore, ANKRD29 is involved in the MAPK signaling pathway, targeting upstream activators or stabilizing its expression via epigenetic modulators may help restore immune homeostasis[53]. Functional studies using ANKRD29-knockout or overexpression models in PD and BC are necessary to confirm its precise role in immune regulation and the tumor microenvironment.

Accumulating evidence has demonstrated that small molecules, particularly microRNAs (miRNAs), play pivotal roles as key regulators of gene expression in various diseases[57]. Targeting specific miRNAs has emerged as a promising strategy for identifying potential biomarkers and therapeutic targets, thereby advancing the development of molecular-based approaches for disease diagnosis and treatment[58]. miRNAs are small non-coding RNAs with significant biological importance, capable of modulating molecular signaling pathways by regulating multiple mRNAs. For instance, miR-21, a miRNA dysregulated in various diseases, has been found to be abnormal in multiple types of stroke, where it plays a crucial role in cell proliferation and apoptosis[58–61]. Furthermore, dysregulation of miRNAs has been observed in preeclampsia (PE), where they may serve as potential biomarkers and therapeutic targets[62]. For example, miRNA-510-3p is upregulated in the blood of PE patients and contributes to vascular dysfunction by targeting vascular endothelial growth factor A (VEGFA) and its signaling axis[63,64]. Similarly, miR-223 exerts anti-inflammatory effects in PE by targeting nod-like receptor pyrin domain-containing 3 (NLRP3)[65]. Additionally, several microRNAs are implicated in the development of both PD and BC, serving as potential biomarkers and therapeutic targets for these diseases[66,67]. These findings

underscore the potential of miRNAs as diagnostic markers and therapeutic targets for complex diseases. In the context of our study, exploring miRNAs that target TDO2 and ANKRD29 may provide novel insights into their regulatory roles in the progression of PD and BC. By modulating the expression of these genes and their associated mRNAs, miRNAs could serve as critical mediators in the crosstalk between these two diseases. In conclusion, targeting TDO2, ANKRD29, or their related miRNAs represents a promising avenue for future research, with potential implications for understanding disease mechanisms and developing targeted therapies.

Our study has several limitations. First, it primarily relied on publicly available transcriptomic datasets, including GEO and TCGA, which, while providing valuable large-scale data, may not fully capture the heterogeneity of PD and BC. These datasets often lack detailed clinical metadata, such as disease severity, treatment history, and comorbidities, which are essential for a more comprehensive understanding of the PD-BC relationship. Additionally, variations in sample collection, processing, and sequencing platforms across datasets could introduce batch effects and potential biases in gene expression analysis. Second, although we validated our findings using qPCR and immunohistochemistry, the validation was performed on a limited number of patient samples, necessitating further validation in larger, independent cohorts. Therefore, future studies should incorporate multi-center prospective cohorts with well-characterized clinical and immunological parameters to allow for more robust validation of the identified biomarkers, ANKRD29 and TDO2, in both PD and BC. Longitudinal studies tracking patients over time could help establish a causal link between chronic inflammation in PD and tumor progression in BC, further strengthening the biological relevance of our findings. Finally, while our study identified associations between ANKRD29, TDO2 and immune regulation in PD and BC, the mechanistic underpinnings remain to be fully elucidated. Future research should include in vivo models and functional assays to confirm causal relationships and identify potential therapeutic targets.

Conclusion

Dysregulation of acid metabolism and immune responses in PD may substantially contribute to the increased risk of BC. TDO2 and ANKRD29 serve as common biomarkers between PD and BC, potentially co-regulating the pathogenesis of both diseases by modulating immune responses and the tumor microenvironment. Chronic inflammation in PD, coupled with altered organic acid metabolism, creates an immunosuppressive environment that facilitates tumor progression in BC. The upregulation of TDO2 and downregulation of ANKRD29 in both conditions suggest a synergistic mechanism underlying their co-occurrence. Furthermore, multiple miRNAs have emerged as key regulators of gene expression in various diseases, with potential to serve as diagnostic biomarkers and therapeutic targets. Targeting miRNAs that modulate TDO2 and ANKRD29 expression could provide new avenues for treatment, offering a strategy to restore immune balance and disrupt tumor progression. Therefore, targeting TDO2, restoring ANKRD29 expression, and exploring miRNA-based therapies may represent promising approaches for managing both PD and BC, with the potential to improve patient outcomes through immune modulation and regulation of the tumor microenvironment.

Data availability

Publicly available datasets were analyzed in this study. This data can be found at TCGA (https://www.cancer.gov/ccg/research/genome-sequencing/tcga) and the GEO data repository (https://www.ncbi.nlm.nih.gov/geo/) and includes the accession numbers: GSE16134, GSE10334, GSE42568 for bulk RNA-seq, and GSE164241 and GSE176078 for scRNA-seq.

Received: 6 December 2024; Accepted: 24 March 2025
Published online: 02 April 2025

References

1. Sheu, J. J. & Lin, H. C. Association between multiple sclerosis and chronic periodontitis: A population-based pilot study. *Eur. J. Neurol.* **20**, 1053–1059. https://doi.org/10.1111/ene.12103 (2013).
2. Ma, C. et al. Periodontitis and stroke: A Mendelian randomization study. *Brain Behav.* **13**, e2888. https://doi.org/10.1002/brb3.2888 (2023).
3. Marouf, N. et al. Association between periodontitis and severity of COVID-19 infection: A case-control study. *J. Clin. Periodontol.* **48**, 483–491. https://doi.org/10.1111/jcpe.13435 (2021).
4. Nwizu, N. N. et al. Periodontal Disease and Incident Cancer Risk among Postmenopausal Women: Results from the Women's Health Initiative Observational Cohort. *Cancer Epidemiol. Biomark. Prev. : A Publ. Am. Assoc. Cancer Res. cosponsored Am. Soc. Prev. Oncol.* **26**, 1255–1265. https://doi.org/10.1158/1055-9965.Epi-17-0212 (2017).
5. Nwizu, N., Wactawski-Wende, J. & Genco, R. J. Periodontal disease and cancer: Epidemiologic studies and possible mechanisms. *Periodontol.* **2000**(83), 213–233. https://doi.org/10.1111/prd.12329 (2020).
6. Bray, F. et al. Global cancer statistics 2018: GLOBOCAN estimates of incidence and mortality worldwide for 36 cancers in 185 countries. *CA: A Cancer j. clin.* **68**, 394–424. https://doi.org/10.3322/caac.21492 (2018).
7. Binder Gallimidi, A. et al. Periodontal pathogens Porphyromonas gingivalis and Fusobacterium nucleatum promote tumor progression in an oral-specific chemical carcinogenesis model. *Oncotarget* **6**, 22613–22623. https://doi.org/10.18632/oncotarget.4209 (2015).
8. Alon-Maimon, T., Mandelboim, O. & Bachrach, G. Fusobacterium nucleatum and cancer. *Periodontol.* **2000**(89), 166–180. https://doi.org/10.1111/prd.12426 (2022).
9. Chen, C. C., Ho, W. L., Lin, C. H. & Chen, H. H. Stratified analysis of the association between periodontitis and female breast cancer based on age, comorbidities and level of urbanization: A population-based nested case-control study. *PLoS ONE* **17**, e0271948. https://doi.org/10.1371/journal.pone.0271948 (2022).
10. Dizdar, O. et al. Increased cancer risk in patients with periodontitis. *Curr. Med. Res. Opin.* **33**, 2195–2200. https://doi.org/10.1080/03007995.2017.1354829 (2017).
11. Shao, J. et al. Periodontal disease and breast Cancer: A Meta-Analysis of 1,73,162 Participants. *Front. Oncol.* **8**, 601. https://doi.org/10.3389/fonc.2018.00601 (2018).

12. Shi, T. et al. Periodontal disease and susceptibility to breast cancer: A meta-analysis of observational studies. *J. Clin. Periodontol.* **45**, 1025–1033. https://doi.org/10.1111/jcpe.12982 (2018).
13. Langfelder, P. & Horvath, S. WGCNA: An R package for weighted correlation network analysis. *BMC Bioinform.* **9**, 559. https://doi.org/10.1186/1471-2105-9-559 (2008).
14. Dennis, G. Jr. et al. DAVID: Database for annotation, visualization, and integrated discovery. *Genome. Biol.* **4**, P3 (2003).
15. Kanehisa, M., Furumichi, M., Tanabe, M., Sato, Y. & Morishima, K. KEGG: New perspectives on genomes, pathways, diseases and drugs. *Nucl. Acid. Res.* **45**, D353-d361. https://doi.org/10.1093/nar/gkw1092 (2017).
16. Wu, T. et al. clusterprofiler 4.0: A universal enrichment tool for interpreting omics data. *Innovation (Cambridge (Mass.))* **2**, 100141. https://doi.org/10.1016/j.xinn.2021.100141 (2021).
17. Jin, S. et al. Inference and analysis of cell-cell communication using Cell Chat. *Nat. Commun.* **12**, 1088. https://doi.org/10.1038/s41467-021-21246-9 (2021).
18. Baima, G. et al. Periodontitis and risk of cancer: Mechanistic evidence. *Periodontol.* https://doi.org/10.1111/prd.12540 (2023).
19. Sung, C. E. et al. Periodontitis, Helicobacter pylori infection, and gastrointestinal tract cancer mortality. *J. Clin. Periodontol.* **49**, 210–220. https://doi.org/10.1111/jcpe.13590 (2022).
20. Chen, X. et al. CXCL8, MMP12, and MMP13 are common biomarkers of periodontitis and oral squamous cell carcinoma. *Oral Dis.* https://doi.org/10.1111/odi.14419 (2022).
21. Yu, X. et al. Short-chain fatty acids from periodontal pathogens suppress histone deacetylases, EZH2, and SUV39H1 to promote Kaposi's sarcoma-associated herpesvirus replication. *J. Virol.* **88**, 4466–4479. https://doi.org/10.1128/jvi.03326-13 (2014).
22. Hajishengallis, G. Periodontitis: From microbial immune subversion to systemic inflammation. *Nat. Rev. Immunol.* **15**, 30–44. https://doi.org/10.1038/nri3785 (2015).
23. Martinez-Outschoorn, U. E., Peiris-Pagés, M., Pestell, R. G., Sotgia, F. & Lisanti, M. P. Cancer metabolism: A therapeutic perspective. *Nat. Rev. Clin. Oncol.* **14**, 11–31. https://doi.org/10.1038/nrclinonc.2016.60 (2017).
24. Baltazar, F. et al. Monocarboxylate transporters as targets and mediators in cancer therapy response. *Histol. Histopathol.* **29**, 1511–1524. https://doi.org/10.14670/hh-29.1511 (2014).
25. Huang, C., Du, W., Ni, Y., Lan, G. & Shi, G. The effect of short-chain fatty acids on M2 macrophages polarization in vitro and in vivo. *Clin. Exp. Immunol.* **207**, 53–64. https://doi.org/10.1093/cei/uxab028 (2022).
26. Yang, W. & Cong, Y. Gut microbiota-derived metabolites in the regulation of host immune responses and immune-related inflammatory diseases. *Cell. Mol. Immunol.* **18**, 866–877. https://doi.org/10.1038/s41423-021-00661-4 (2021).
27. Li, W., Huang, B., Liu, K., Hou, J. & Meng, H. Upregulated leptin in periodontitis promotes inflammatory cytokine expression in periodontal ligament cells. *J. Periodontol.* **86**, 917–926. https://doi.org/10.1902/jop.2015.150030 (2015).
28. García-Estevez, L., González-Martínez, S. & Moreno-Bueno, G. The leptin axis and its association with the adaptive immune system in breast cancer. *Front. Immunol.* **12**, 784823. https://doi.org/10.3389/fimmu.2021.784823 (2021).
29. Blasco-Baque, V. et al. Periodontitis induced by Porphyromonas gingivalis drives periodontal microbiota dysbiosis and insulin resistance via an impaired adaptive immune response. *Gut* **66**, 872–885. https://doi.org/10.1136/gutjnl-2015-309897 (2017).
30. Biello, F. et al. Insulin/IGF axis in breast cancer: Clinical evidence and translational insights. *Biomolecules* **11**, 125. https://doi.org/10.3390/biom11010125 (2021).
31. Li, Y. et al. Single-cell landscape reveals active cell subtypes and their interaction in the tumor microenvironment of gastric cancer. *Theranostics* **12**, 3818–3833. https://doi.org/10.7150/thno.71833 (2022).
32. Qing, X. et al. Molecular characteristics, clinical significance, and cancer immune interactions of angiogenesis-associated genes in gastric cancer. *Front. Immunol.* **13**, 843077. https://doi.org/10.3389/fimmu.2022.843077 (2022).
33. Dieci, M. V., Miglietta, F. & Guarneri, V. Immune infiltrates in breast cancer: Recent updates and clinical implications. *Cells* **10**, 223. https://doi.org/10.3390/cells10020223 (2021).
34. Kumar, T. et al. A spatially resolved single-cell genomic atlas of the adult human breast. *Nature* **620**, 181–191. https://doi.org/10.1038/s41586-023-06252-9 (2023).
35. Kresovich, J. K. et al. Prediagnostic immune cell profiles and breast cancer. *JAMA Netw. Open* **3**, e1919536. https://doi.org/10.1001/jamanetworkopen.2019.19536 (2020).
36. Kobayashi, R. et al. Induction of IL-10-producing CD4+ T-cells in chronic periodontitis. *J. Dent. Res.* **90**, 653–658. https://doi.org/10.1177/0022034510397838 (2011).
37. Sakaguchi, S. Naturally arising CD4+ regulatory t cells for immunologic self-tolerance and negative control of immune responses. *Annu. Rev. Immunol.* **22**, 531–562. https://doi.org/10.1146/annurev.immunol.21.120601.141122 (2004).
38. Nakajima, T. et al. Regulatory T-cells infiltrate periodontal disease tissues. *J. Dent. Res.* **84**, 639–643. https://doi.org/10.1177/154405910508400711 (2005).
39. Li, C., Yang, T., Yuan, Y., Wen, R. & Yu, H. Bioinformatic analysis of hub markers and immune cell infiltration characteristics of gastric cancer. *Front. Immunol.* **14**, 1202529. https://doi.org/10.3389/fimmu.2023.1202529 (2023).
40. Kostic, A. D. et al. Fusobacterium nucleatum potentiates intestinal tumorigenesis and modulates the tumor-immune microenvironment. *Cell Host. Microb.* **14**, 207–215. https://doi.org/10.1016/j.chom.2013.07.007 (2013).
41. Chen, Y., Zhang, S., Wang, Q. & Zhang, X. Tumor-recruited M2 macrophages promote gastric and breast cancer metastasis via M2 macrophage-secreted CHI3L1 protein. *J. Hematol. Oncol.* **10**, 36. https://doi.org/10.1186/s13045-017-0408-0 (2017).
42. Carrion, J. et al. Microbial carriage state of peripheral blood dendritic cells (DCs) in chronic periodontitis influences DC differentiation, atherogenic potential. *J. immunol. (Baltimore, Md. : 1950)* **189**, 3178–3187. https://doi.org/10.4049/jimmunol.1201053 (2012).
43. De Sanctis, F. et al. MDSCs in cancer: Conceiving new prognostic and therapeutic targets. *Biochem. Biophys. Acta.* **35–48**, 2016. https://doi.org/10.1016/j.bbcan.2015.08.001 (1865).
44. Van der Merwe, M., Van Niekerk, G., Botha, A. & Engelbrecht, A. M. The onco-immunological implications of fusobacterium nucleatum in breast cancer. *Immunol. Lett.* **232**, 60–66. https://doi.org/10.1016/j.imlet.2021.02.007 (2021).
45. Cheng, R. et al. Periodontal inflammation recruits distant metastatic breast cancer cells by increasing myeloid-derived suppressor cells. *Oncogene* **39**, 1543–1556. https://doi.org/10.1038/s41388-019-1084-z (2020).
46. Su, L., Xu, Q., Zhang, P., Michalek, S. M. & Katz, J. Phenotype and function of myeloid-derived suppressor cells induced by porphyromonas gingivalis infection. *Infect Immune* https://doi.org/10.1128/iai.00213-17 (2017).
47. Peck, K. A. et al. Extracellular vesicles secreted by TDO2-augmented fibroblasts regulate pro-inflammatory response in macrophages. *Front. cell Dev. Boil.* **9**, 733354. https://doi.org/10.3389/fcell.2021.733354 (2021).
48. Myint, A. M. et al. Kynurenine pathway in major depression: Evidence of impaired neuroprotection. *J. Affect. Disord.* **98**, 143–151. https://doi.org/10.1016/j.jad.2006.07.013 (2007).
49. Xue, C. et al. Tryptophan metabolism in health and disease. *Cell Metab.* **35**, 1304–1326. https://doi.org/10.1016/j.cmet.2023.06.004 (2023).
50. Zheng, T. et al. Gankyrin promotes tumor growth and metastasis through activation of IL-6/STAT3 signaling in human cholangiocarcinoma. *Hepatol. (Baltimore, Md.)* **59**, 935–946. https://doi.org/10.1002/hep.26705 (2014).
51. Liu, W. B. et al. Epigenetic regulation of ANKRD18B in lung cancer. *Mol. Carcinog.* **54**, 312–321. https://doi.org/10.1002/mc.22101 (2015).
52. Wu, Y., Liu, H., Gong, Y., Zhang, B. & Chen, W. ANKRD22 enhances breast cancer cell malignancy by activating the Wnt/β-catenin pathway via modulating NuSAP1 expression. *Bosn. J. Basic. Med. Sci.* **21**, 294–304. https://doi.org/10.17305/bjbms.2020.4701 (2021).

53. Zhao, H. et al. ANKRD29, as a new prognostic and immunological biomarker of non-small cell lung cancer, inhibits cell growth and migration by regulating MAPK signaling pathway. *Biol. Direct* **18**, 28. https://doi.org/10.1186/s13062-023-00385-7 (2023).
54. Song, H. et al. Construction of a circRNA-Related ceRNA prognostic regulatory network in breast cancer. *Onco. Target. Ther.* **13**, 8347–8358. https://doi.org/10.2147/ott.S266507 (2020).
55. Fox, E. et al. Indoximod: An immunometabolic adjuvant that empowers T cell activity in cancer. *Front. Oncol.* **8**, 370. https://doi.org/10.3389/fonc.2018.00370 (2018).
56. Hu, S. et al. TDO2+ myofibroblasts mediate immune suppression in malignant transformation of squamous cell carcinoma. *J. clin. Investing.* https://doi.org/10.1172/jci157649 (2022).
57. Saliminejad, K., Khorram Khorshid, H. R., Soleymani Fard, S. & Ghaffari, S. H. An overview of microRNAs: Biology, functions, therapeutics, and analysis methods. *J.cell. physiol.* **234**, 5451–5465. https://doi.org/10.1002/jcp.27486 (2019).
58. Sekar, D., Venugopal, B., Sekar, P. & Ramalingam, K. Role of microRNA 21 in diabetes and associated/related diseases. *Gene* **582**, 14–18. https://doi.org/10.1016/j.gene.2016.01.039 (2016).
59. Panagal, M. et al. Dissecting the role of miR-21 in different types of stroke. *Gene* **681**, 69–72. https://doi.org/10.1016/j.gene.2018.09.048 (2019).
60. Sekar, D., Shilpa, B. R. & Das, A. J. Relevance of microRNA 21 in different types of hypertension. *Curr. Hypertens. Rep.* **19**, 57. https://doi.org/10.1007/s11906-017-0752-z (2017).
61. Panagal, M. et al. MicroRNA21 and the various types of myeloid leukemia. *Cancer Gene Ther.* **25**, 161–166. https://doi.org/10.1038/s41417-018-0025-2 (2018).
62. Selvakumar, S. C., Preethi, K. A., Ross, K. & Sekar, D. The emerging role of microRNA-based therapeutics in the treatment of preeclampsia. *Placenta* **158**, 38–47. https://doi.org/10.1016/j.placenta.2024.09.018 (2024).
63. Sekar, D., Lakshmanan, G., Mani, P. & Biruntha, M. Methylation-dependent circulating microRNA 510 in preeclampsia patients. *Hypertens. Res.: Off. J. Jpn. Soc. Hypertens.* **42**, 1647–1648. https://doi.org/10.1038/s41440-019-0269-8 (2019).
64. Selvakumar, S. C., Preethi, K. A. & Sekar, D. MicroRNA-510-3p regulated vascular dysfunction in preeclampsia by targeting vascular endothelial growth factor a (VEGFA) and its signaling axis. *Placenta* **153**, 31–52. https://doi.org/10.1016/j.placenta.2024.05.135 (2024).
65. Liu, X., Li, Z. & Lu, D. MicroRNA-223-3p downregulates the inflammatory response in preeclampsia placenta via targeting NLRP3. *BMC Pregnancy Childbirth* **24**, 175. https://doi.org/10.1186/s12884-024-06371-9 (2024).
66. Xu, X., Lang, G. P., Chen, Z. L., Wang, J. L. & Han, Y. Y. The dual role of Non-coding RNAs in the development of periodontitis. *Biomed. Environ. Sci.: BES* **36**, 743–755. https://doi.org/10.3967/bes2023.079 (2023).
67. Kandettu, A., Radhakrishnan, R., Chakrabarty, S., Sriharikrishnaa, S. & Kabekkodu, S. P. The emerging role of miRNA clusters in breast cancer progression Biochimica et biophysica acta. *Rev. cancer.* **1874**, 188413. https://doi.org/10.1016/j.bbcan.2020.188413 (2020).

Acknowledgements

The authors thank the GEO and TCGA databases for the information provided.

Author contributions

All authors have made substantial contributions to the conception and design of the study. Erli Wu and Wei Shao designed the project and wrote the manuscript. Jiahui Liang, Jingxin Zhao, Feihan Gu, Yuanyuan Zhang, Biao Hong performed collection and/or assembly of data, data analysis, and interpretation. Qingqing Wang, Wei Shao and Xiaoyu Sun gave final approval of manuscript and financial support. All authors read and approved the final manuscript.

Funding

This work was supported by the National Natural Science Foundation of China (82071770); Research Level Improvement Project of Anhui Medical University (2021xkjT001);Basic and Clinical Cooperative Research and Promotion Program of Anhui Medical University (2021xkjt039); Natural Science Foundation of Anhui Province (2208085QH245); the National Natural Science Foundation of China (82201127); Research Program of Natural Science Foundation of Anhui Higher Education Institutions (KJ2021A0273) and Anhui Medical University Stomatological Hospital "Feng Yuan Cooperation" Program (2022xkfyhz06).

Declarations

Competing interests

The authors declare no competing interests.

Ethics approval and consent to participate

This study was approved by Anhui Medical University Affiliated Stomatology Hospital Ethics Committee (Ethics number: 2021006), and informed consent has been signed by all participants. All methods were performed in accordance with relevant guidelines and regulations.

Additional information

Supplementary Information The online version contains supplementary material available at https://doi.org/10.1038/s41598-025-95703-6.

Correspondence and requests for materials should be addressed to Q.W., W.S. or X.S.